Developing Pulse Phase Thermography as a Characterisation Tool for Grossly Sculpted Surfaces

Ang, K.C., Wood, R.J.K., Wang, L., Dulieu-Barton, J.M.,
University of Southampton, Southampton, SO17 1BJ, United Kingdom
Dance, B.G.I., Buxton, A.L., TWI Ltd, Cambridge, CB21 6AL, United Kingdom

This paper presents the capabilities of a novel direct-writing electron-beam (EB) process and describes some initial work to develop pulse phase thermography (PPT) as a surface characterisation tool for geometrical features sculpted by this process. A concise review of existing rough surface characterisation techniques found no commonly accepted surface characterisation method for such grossly textured surfaces. Consequently, the potential of existing thermal technology and in particular PPT is explored in the context of developing a methodology to characterise the EB sculpted surface features. Initial tests using PPT on blind holes with various depths to simulate gross surface features are reported and used to determine the feasibility of this method for surface feature recognition and measurement. The paper also outlines proposals to extend PPT for protrusions and pits of different heights and depths measurements as a novel step forward to develop a sophisticated quality assessment (QA) tool. Scanning electron microscopy (SEM) and micro computed tomography (CT) are used as a reference to assess the accuracy of the three-dimensional surface topographical results obtained by PPT.

For more information contact:
Kang Cheng Ang
University of Southampton
3011, Eustice Building
Southampton
SO17 1BJ United Kingdom
Phone – 0044 (0)2380598331
E-mail – kca@soton.ac.uk

The Direct-Writing EB Process Background and Surface Characterisation

The novel *Surfi-Sculpt*® direct writing EB process has been recently developed and involves fast repeated displacement of material on the surface with an intense beam of electrons[1-3]. Surfaces are both melted and partially vaporised with the EB. Both surface tension and vapour pressure forces help to move molten material in a controlled fashion. Repeated visits of the beam generate surface features within the treated region. Fast rastering can process an area of $25 \times 25 mm^2$ within a fraction of a second. Complex surface features including protrusions or pits into the surface of materials including stainless steel, aluminium, titanium and nickel based alloys can be manufactured that range in size from a few tens of microns to several millimetres high or deep. These features can have an aspect ratio of the order of 10:1 (height to width). Thus, these types of surface can be categorized as extraordinary rough. The rough surfaces can be tailored to meet specific requirements such as those required to facilitate joints in materials that have application in major industries like aerospace, automotive, electronics and medical. However, a reliable method of assessment of the quality of EB sculpted surfaces has not been forthcoming. The repeatability and accuracy of the features, is of primary importance, therefore, the aim of this investigation is to develop techniques that allow accurate measurement of the EB features.

In this paper characterisation techniques for rough surfaces are reviewed and preliminary tests are carried out to explore their capabilities for measuring EB sculpted surface features. The geometric characterisation of the EB rough features is challenging due to the small scale, complex shape, and large angles of obliquity and overhangs/keyholes. One of the candidate technologies, PPT, which has primarily been used for defect detection, is explored for surface characterisation especially on subsurface features for the first time in this study. A detailed description of the application of PPT for assessment of rough surfaces is presented in this paper.

EB Surfaces Characterisation Requirements

Typically the rough surfaces produced by the EB process include features such as spikes, burr-free holes, blades, channels and swirls. Dimensions such as the height, width and angle of the features are required so that the geometries of the features are fully defined. These extraordinarily rough features require measurements within the range of 0.5-2mm ± 0.1mm in height/depth. Fig. 1 (a) and (b) shows the topography of a relatively simple sculpted surface from SEM and micro CT respectively. These two surface characterisation methods are being used as reference techniques due to their high resolution and subsurface imaging capability. However, it is considered that neither of these techniques is suitable for use in a production environment due to their relatively high cost, size limitations on test samples and their requirement to operate in a vacuum.

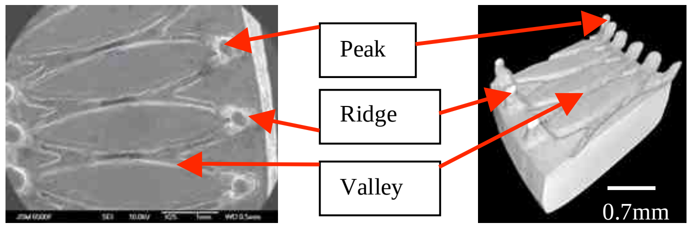

(a) *(b)*

Fig.1 – (a) SEM and (b) CT images of an EB sculpted surface

Review of Surface Characterisation Techniques for Rough Surfaces

A concise review of existing rough surface characterisation techniques shows that all techniques can be divided into contact techniques which employ styli or non-contact techniques based on various technologies such as optical, electronmicroscopy, tomography, thermography and ultrasound. One contact and nine non-contact methods based on different working principles are reviewed, tested and summarised in Table 1. A review of these techniques has shown no single system can provide all of the information required to define the surface geometry. Based on the advantages and disadvantages of the techniques' with reference to EB surfaces, it is clear that a new approach is needed to allow a suitable surface characterisation tool to be developed.

Contact Measurement Techniques

Whitehouse pointed out that all surface measurement techniques are analogous to two natural means of assessment: either through touch by running a finger over the surface or by simple visual examination[4]. Contact techniques are the embodiment of the former. One recently developed technique, coordinate-measuring (see Table 1–A) is a good example of a 3-D stylus system used for dimensional measuring. Three axes coordinate data points of measured surfaces are easily produced with the 3-D stylus system. Subsequently, geometric measurements are achieved on the reconstructed 3-D model based on the data points.

Non-Contact Measurement Techniques

Non-contact measurement techniques replace the physical contact of a stylus with optics and sensors that focus onto the surface and are sensitive to white light, laser beams, electrons, X-rays, thermal, or ultrasound.

Optical techniques

All the optical techniques described here involve projecting light onto a surface. The four main optical methods include focus detection, interferometry, light scattering, and the recently developed technique of focus variation. Machine vision is also included as an extension of the optical methods.

Focus detection instruments perform measurements by maintaining the optical focus. Numerous methods have been developed to obtain sharp optical focus by varying the focus detection mechanism, vertical and horizontal scans. The **confocal** method (see Table 1–B) is by far the most promising focus detection technique because of the capability to give submicron resolution. .

The application of **interferometry** to surface measurement started after Michelson invented the interferometer in the 19th century. A series of 'fringes' are produced consisting of parallel bands produced by interference of light waves[5]. Laser phase shifting[6] (see Table 1–C) and white light scanning differential interferometry[7] are the two commonly used 3-D surface topography methods. These methods utilize the interference patterns obtained from two reflected beams, one from the sample surface and one from a reference mirror in order to distinguish the sample surface topography. In addition, combining the two techniques has resulted in a compromise between the resolution and performance[8].

Light scattering is a technique that utilizes the **triangulation** method, by focusing a laser spot of 30μm dia. on the surface and analysing the light scattered from the interaction of the laser beam and the surface. Slazas described that there are two main configurations being used in laser triangulation, namely specular and diffuse (see Table 1–D), depending on the direction of the incoming light[9].

Innovative combinations of techniques with small depths of focus and vertical scanning capability have recently led to the introduction of **focus variation** techniques. The method (see Table 1–E) employs coaxial white light focused onto the surface and the reflected light is then projected onto a colour digital sensor to provide both the topographical and true colour information of the sample surface[10].

Machine vision technology (see Table 1–F) employs a microcomputer-based vision system to register the pattern of scattered light from the surface to derive the surface information[11,12]. This is a fast imaging technique that utilizes one or multiple light sources to obtain images without scanning procedures.

Optical technologies have shown potential for scanning and measurement of 3-D complex surfaces. However, the line-of-sight and light wavelength principles may limit the application of the optical methods in analysing EB surfaces especially those with steep slopes and undercut features. Shadow effects due to limited reflection of the light from the surfaces can limit the effective reconstruction of grossly deformed or rough surfaces.

Scanning Microscopy

Scanning electron microscope (SEM) (see Table 1–G) was invented in 1938 and is the most common system in this scanning microscopy category[13]. Stereo pairs of SEM images obtained by tilting the sample at different angles provide some measurements of the surface topography. One important consideration on the reconstruction of 3-D model is the 100% dependency on the 2-D SEM images. Therefore, tailored optimisation of suitable SEM variables such as the working distance, and tilting angle is required.

Tomography

Tomography is an imaging technique that is widely used in the medical field enabling non-invasive 3-D imaging of objects through reconstruction of 2-D images. The quotation from Galileo Galilei "to make measurable the things that are not" introduced the concept of tomography. The ability to reveal internal defects that are not visible externally is the main motivation to use the tomography in Non-Destructive Evaluation (NDE). To do this in metallic structures, a high power X-ray source is used to reveal the defects which are then mapped to produce their 3D geometry using computed tomography (CT)[14]. CT (see Table 1–H) involves the acquisition of a large number of radiographic projections while a specimen is rotated. CT has the potential for a breakthrough in the measurement of EB surfaces as internal measurements such as pits.

Thermography

Infrared (IR) **thermography** is a combination of the typical optical systems with the penetration capability of thermal radiation into the test samples. The technology originated when William Herschel discovered thermal radiation IR[15]. Pulse Thermography (PT) and Modulated Thermography (MT) are the two fundamental techniques in this category. Pulse Phase Thermography (PPT) (see Table 1–I) is a relatively new approach that unites the advantages of the two fundamental approaches such as fast data acquisition and generation of phase data that are not sensitive to the non-uniformities of heating, surface emissivity variations, surface geometries and reflections from the environment in comparison to the typical amplitude data[16].

Since its introduction, PPT has been used to examine defects and detect damage in a wide range of materials such as metals, plastics, plasters, woods, and composite structures[17]. Therefore the technique can be applied to the metallic materials used to produce the EB surfaces. The technique has the advantage in that it can reveal subsurface data and because it is essentially measuring the rate of heat transfer, the technique does not require full optical accessibility. The techniques precision must be obtained on terms of being able to derive geometrical information. Furthermore its applicability at relatively small scales of submicron has not been established.

Ultrasound

Ultrasound back scattering (see Table 1–J) is another option to measure surface topography of a sample surface based on wave travel between the transducer and the surface[18]. With the typical range of frequency between 1MHz and 30MHz, the method has the advantage to reveal subsurface features. However, according to the ultrasound propagation properties, the wavelengths in this range of frequencies are around 1.5mm. Therefore, the resolution of this method may not be sufficient for EB surfaces.

Table 1 – Contact and non-contact principles and their feasibility studies

Techniques		Schematic Diagram	Principles	Advantages/limitations for EB surfaces
A	Coordinate-Measuring Machine (CMM)[19]	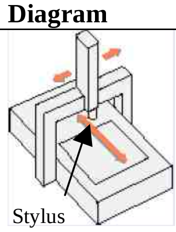	Contact + profiling with stylus	-capable to produce good z axis resolution of ±0.5µm -able to measure positive surfaces with best accuracy of few microns -300µm stylus size limitation to negative surfaces such as holes, high cost when using the newest 30µm diameter stylus -need to be in contact with surfaces
B	Focus Detection (Confocal)[20-22]	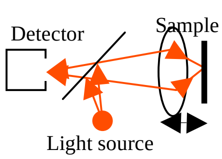	Non-contact + optical point source laser or white light + in-focus light maintained	-capable to produce good resolution of ±0.1µm -for fairly small features of few microns & smooth surfaces of 10-15° slope

C	Interferometry (Phase-shifting)[23]	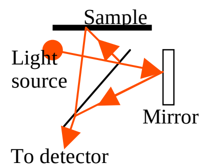	Non-contact + optical narrow band laser source + light interference	-capable to produce best z axis resolution of ± 0.1nm -for very small features -limited to high reflectivity surfaces
D	Light Scattering (Laser triangulation)[24-26]	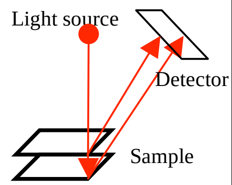	Non-contact + optical point source or line laser + light scattered detection	-capable to produce good z axis resolution of ±1µm -good for relatively large features of tenths microns -has large angular measurements to cope with random surfaces -relatively low cost
E	Focus Variation[10, 27]	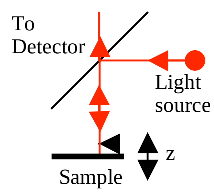	Non-contact + optical white light source + focus point variation	-capable to produce good z axis resolution of ±0.2-2µm -has good angular measurements to handle rapid steep slopes up to 80° -relatively expensive
F	Machine Vision[11, 28]	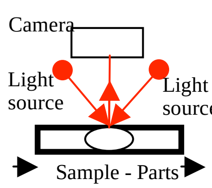	Non-contact + optical white light or laser pattern + imaging	-capable to produce good z axis resolution of ±0.1µm -involves fast imaging -limited accuracy to reconstruct 3-D images for measurements
G	Scanning microscopy (Scanning electron microscopy - SEM)[13, 29-30]	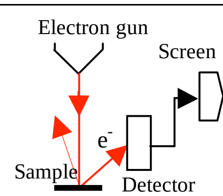	Non-contact + beam of electrons + secondary electrons intensity detection	-capable to produce best z axis resolution of ±5nm -vacuum environment is required -require sample preparation due to sample holder limitation
H	Tomography (Micro Computed Tomography – MicroCT)[14, 31]	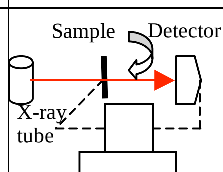	Non-contact + beam of x-rays + X-rays intensity detection	-capable to produce good z axis resolution of ±5µm -possibility of detecting holes and undercut features -detectable sample size is limited based on the material types
I	Thermography (Pulse Phase Thermography – PPT)[15-16]	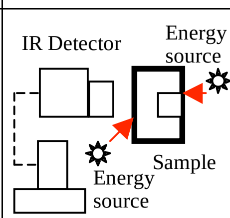	Non-contact + heat pulse + surface temperature changes detection	-able to produce thermal resolution of ±2mK -involves fast imaging -possibility of detecting holes and undercut features -surfaces need to be painted

J	Ultrasound[32-33]	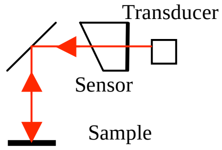	Non-contact + ultrasound pulses + ultrasound pulses reflection	-produce resolutions of few hundreds microns -wavelength (millimeters) of ultrasound is too large to characterize sculpted features

From the survey and preliminary testing on the ten listed techniques, the PPT technique has been chosen for further investigation as a possible quality assurance tool to characterize sculpted surfaces. PPT is selected based on its technical capabilities such as fast imaging and visualisation of features in the underlying materials.

Pulse Phase Thermography

Pulse Phase Thermography (PPT) is a relatively new approach in field of thermal non-destructive testing and evaluation[16]. Generally, the technique employs an infrared detector to record the surface temperature changes when the test sample is heated using a pulsed heat source such as photographic flash. In PPT, a short pulse of heat from an energy source is applied to the sample surface while the thermal data collected by the infrared detector is analysed by applying a Fourier Transform (FT) that provides phase delay images.

The test sample can be heated from one side while thermal data is collected either from the same side, or from the opposite side. The former hardware configuration is classified as *reflection mode* while the latter is termed *transmission mode*. Both modes compromise on the resolution and height/depth of features detection. The reflection mode is usually used when inspecting features closer to the surface, whereas transmission is favoured for detecting features that are deeper inside the component[15, 34].

The infrared detection system is such that it can collect multiple images per second, allowing a time history to be developed with respect to the heat pulse. These thermal images are then computed as phase and amplitude images in the frequency domain through Discrete Fourier Transform (DFT). The derivation of DFT is[35-36]:

$$F_n = \Delta t \sum_{k=0}^{N-1} T(k\Delta t) \exp^{\left(\frac{-j^2 \pi n k}{N}\right)} = \mathrm{Re}_n + \mathrm{Im}_n \qquad (1)$$

where F is the symbol for Fourier transform, Δt is the sampling interval, T is the temperature and k is the sequence of complex numbers ($k=0,\ldots, k=N-1$). The computed amplitude and phase are expressed as follows:

$$\mathrm{Re}_n = A_n \cos\phi_n \quad (2)$$

$$\mathrm{Im}_n = A_n \sin\phi_n \quad (3)$$

Or equivalently:

$$A_n = \sqrt{\mathrm{Im}_n{}^2 + \mathrm{Re}_n{}^2} \quad (4)$$

$$\phi_n = \tan^{-1}\left(\frac{\mathrm{Im}_n}{\mathrm{Re}_n}\right) \quad (5)$$

Phase images are quantified with the analysis of blind frequency concept to distinguish different features of depth[37]. The blind frequency is defined as the frequency for which a feature at a particular depth becomes primarily evident in the frequency spectrum. The defined blind frequency can be estimated with another important element, $\Delta\phi$, and the phase contrast which is defined[38], as:

$$\Delta\phi = \phi_{\mathrm{d}} - \phi_{\mathrm{s}} \quad (6)$$

where $\Delta\phi$ is the phase contrast, ϕ_d is the phase that can be associated with a 'feature' and ϕ_s is the phase associated with a surface without a feature, referred to in damage analysis as the 'sound' phase but in this paper as the 'non-feature' phase. The blind frequency is established when there is no significant phase contrast. The blind frequency is then subsequently related to the diffusion length equation[15] and the phase delay definition[38].

The respective thermal diffusion length and phase delay equations are:

$$\mu = \sqrt{\frac{2\alpha}{\omega}} \quad (7)$$

$$\phi = \frac{z}{\mu} \quad (8)$$

where μ is the thermal diffusion length, α is the thermal diffusivity, ω is the angular frequency, ϕ is the phase, and z is the depth of features. The thermal diffusivity associated with a surface without a feature is formulated as follows:

$$\alpha_s = \frac{k}{\rho C_p} \qquad (9)$$

where α_s is the thermal diffusivity for the 'non-feature' surface, k is the thermal conductivity for the sample, ρ is the density for the sample, and C_p is the specific heat capacity for the sample. Therefore, depth of the features can be related to the blind frequency in the following manner:

$$z \propto \phi_s \sqrt{\frac{\alpha_s}{\pi f_b}} \qquad (10)$$

where f_b is the blind frequency.

Preliminary PPT Experimental Tests and Results

Fig. 2 shows an aluminium test sample with an array of blind holes of different depths fabricated for the early PPT testing. The experimental setup for this early PPT testing is as illustrated in Table 1–I. The PPT testing developed in this work can be divided into four important stages; data acquisition, the Fourier transform, feature identification, and feature characterisation. For the acquisition stage, the hardware configuration, the sample preparation, experimental parameters selection and experimental modes are crucial elements. After proper consideration of the elements in the first stage, a series of thermal images of the surface temperature evolution are captured using an infrared detector system and inputted to the Fourier transform stage. Phase and amplitude images are the outputs from this second stage using equations (1), (2), (3), (4), and (5). Subsequently, from the phase images, feature identification is performed. In the feature identification stage, thermal data retrieved is normalised to obtain the statistical mean that reduces uncertainties such as heat inhomogeneity at different locations on the sample and random noise level. Finally, an analysis and mathematical computations based on the phase data, blind frequency, and sample thermal properties are conducted at the feature characterisation stage using equations (6), (7), (8), (9), and (10). Fig. 3 illustrates the four stages of PPT testing involved.

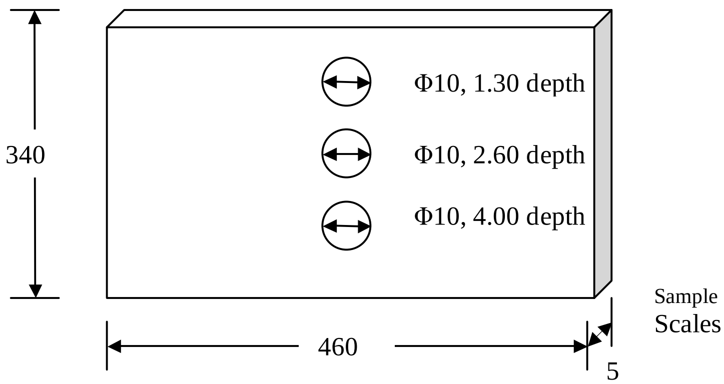

Fig. 2 – Test Sample with Array of Blind Holes

Comparisons of initial results for actual and characterised feature depths are shown in Table 2 while Fig. 4 illustrates the thermal phase image achieved. The PPT tests show encouraging results for both the qualitative and quantitative characterisation. In this initial work phase, transmission and reflection modes were examined with the objective to provide some confidence levels for further development of PPT to characterise the EB surfaces. The initial feasibility shows that transmission mode is possibly more favourable for characterisation of complex features due to the smaller measurement errors obtained when compared to the larger errors in reflection mode. However, further in-depth studies on the random variables that would influence the identification of the phase data such as the level of noise in the data, the inhomogeneity of internal sample surface structures, and the inhomogeneity of surface emissivity especially of the black matt paint are crucial to obtain a good resolution for measuring the depth of the features.

Acquisition

Hardware:

1. FPA Infrared Camera of a 320 x 256 pixels array with 269 Hz maximum frame rate
2. Electronic flash unit giving 0.6 ms duration, 17 Watt-hours energy, and normal daylight temperature per heat pulse

Sample Preparation:

Aluminium test sample of 460 mm x 340 mm x 5 mm with 10 mm diameter of complex blind holes at different depths 1.30 mm, 2.60 mm, and 4.00 mm is painted with high temperature black matt aerosol paint.

Experimental Parameters:

1. Frame rate: 269Hz
2. Integration time: 3700µs
3. No. of frames captured per video: 1000 frames

Experimental Modes:

a. Transmission
b. Reflection

⇩

Fourier Transform

Thermographic video consisting of 1000 sequential images is analysed using equation (1) of Discrete Fourier Transform in the infrared system. A series of amplitude and phase images as formulated in equations (2), (3), (4) and (5) are generated from the function.

⇩

Feature Identification

Phase data of 120 pixels for feature and undamaged area of the sample are retrieved from each phase images. The retrieved data points are then normalised to obtain the statistical mean.

⇩

Feature Characterisation

The normalised phase information from each captured phase images are plotted as phase contrast versus frequency graphs. Blind frequencies are determined when no significant phase contrast can be observed. Blind frequencies together with sample thermal properties of thermal conductivity, $k_{Al} = 237\ Wm^{-1}K^{-1}$, density, $\rho_{Al} = 2700\ kgm^{-3}$, and specific heat capacity, $Cp_{Al} = 897\ Jkg^{-1}K^{-1}$ are used for feature depth determination using equations (6), (7), (8), (9) and (10).

Fig. 3 – Four stages of PPT testing

Table 2 – Comparison of Results for Actual and Characterised Feature Depths

Feature Actual Depth, ± 0.02 (mm)	Experiment Mode	Average Sound Phase, ϕ_s (rad)	Blind Frequency, f_b (Hz)	Feature Characterised Depth, z (mm)	Error (%) [(Actual – Characterised) /Actual]
4.00	Transmission	0.38	0.40	3.40	15
	Reflection	0.18	0.39	3.40	15
2.60	Transmission	0.14	0.28	1.48	43
	Reflection	0.51	0.44	4.29	65
1.30	Transmission	0.17	0.47	1.43	10
	Reflection	0.07	0.31	0.67	48

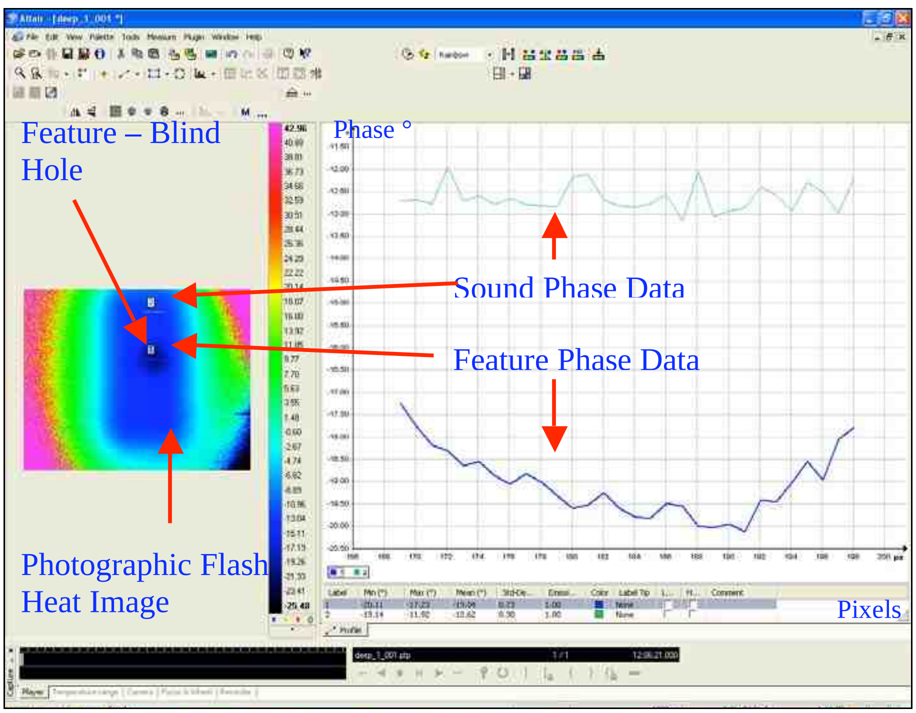

Fig. 4 – Thermal Phase Image

Conclusions

This paper details the development of PPT as a potential characterisation tool for rough EB sculpted surfaces. The next step in the process is to apply PPT to EB features. Apart from the hardware development, in the future this study will also develop an integrated software system which can fully represent the features. SEM and microCT will be extended as well to assess the submicron accuracy of the three-dimensional surface topographical results obtained by PPT.

Acknowledgements

University of Southampton is one of the partners in the DTI ASTIA project together with four industrial partners – TWI Ltd., Symmetry Medical, Aquasium and Henkel Technologies. This part of work in ASTIA was fully supported by EPSRC.

References

[1] B.G.I. Dance, International Patent Publication Number WO 2002/094497 A3, Modulated Surface Modification (2002).
[2] B.G.I. Dance, E.J.C. Kellar, International Patent Publication Number WO 2004/028731 A1, Workpiece Structure Modification (2004).
[3] A.L. Buxton, B.G.I. Dance, Proc. 4th International Surface Engineering Congress, p. 107 (2005).
[4] D.J. Whitehouse, Handbook of surface metrology, Institute of Physics Publishing, Bristol, 1994; p.1.
[5] P. Hariharan, Interferometers, Handbook of Optics, McGraw-Hill Companies, Inc., New York, 1996; p.21.
[6] D.M. Perry, P.J. Moran, G.M. Robinson, J. IERE, **55**, 145 (1985).
[7] G. Makosch, B. Drollinger, Applied Optics, **23**, 4544 (1984).
[8] P.J. Caber, S.J. Martinek, R.J. Niemann, Proc. SPIE. p. 2088 (1993).
[9] P.A. Slazas, Sensor Review, **16**, 33 (1996).
[10] R. Danzl, F. Helmli, Proc. 6th International Euspen Conference, p. 516 (2006).
[11] N., Zuech, Understanding and Applying Machine Vision, Marcel Dekker, Inc., 2000; p. 1.
[12] F. Luk, V. Huynh, W. North, J. Phys. E: Sci. Instrum., **22**, 970 (1989).
[13] P.J. Goodhew, J. Humphreys, R. Beanland, Electron Microscopy and Analysis, Taylor & Francis, London, 2001; p. 1.
[14] P. Wenig, S. Kasperl, Proc. 9th ECNDT, p. 1 (2006).
[15] X. Maldague, Theory and Practice of Infrared Technology for Non-Destructive Testing, John Wiley & Sons, Inc, 2001; p. 1.
[16] X. Maldague, S. Marinetti, Journal of Applied Physics **79**, 2694 (1996).

[17] X., Maldague, S., Marinetti, J.P., Couturier, Review of Progress in QNDE, p. 339 (1997).
[18] M. Miller, B. Mi, A. Kita, I.C. Ume, Mechatronics, **12**, 1259 (2005).
[19] R.N. Frank, Proc. Interagency Mechanical Operations Group (IMOG) gauging subgroup conference, p. 1 (1992).
[20] M. Minsky, United States patent 3013467 (1961).
[21] D.K. Hamilton, T. Wilson, Applied Physics B, **27**, 211 (1982).
[22] T. Wilson, Journal of Microscopy, **153**, 161 (1989).
[23] A. Harasaki, J. Schmit, J.C. Wyant, Applied Optics **39**, 2107 (2000).
[24] P. Beckman, Progress in Optics **6**, 53 (1967).
[25] M.C. Pires, J.P. Coelho, M.A. Abreu, Handbook on the Use of Lasers in Conservation and Conservation Science, COST office, Brussels, Belgium, 2006; p. 3.
[26] M. Costa, Proc. SPIE 2248, p. 151 (1994).
[27] R. Danzl, 3-D Measurement using a colour focus sensor, Guidelines to Inspection of Surfaces with Image Processing, ISBN 3-8167-7061-4 (2006).
[28] G.A. Al-Kindi, R.M. Baul, K.F. Gill, International Journal of Production Research **30**, 241 (1992).
[29] M. Hemmleb, M. Schubert, Proc. 2nd Turkish-German Joint Geodetic Days, p. 745 (1997).
[30] J.H. Lee, J.C. Russ, Journal of Computer-assisted Microscopy **1**, 79 (1989).
[31] R.A. Ketcham, W.D. Carlson, Computers and Geosciences **27**, 381 (2001).
[32] G.V. Blessing, D.G. Eitzen, Surface Topography **1**, 253 (1988).
[33] J. Jaros, J. Rozman, Measurement Science Review **4**, 27 (2004).
[34] X. Maldague, J-P. Couturier, Proc. 4th International Workshop on Advanced Infrared Technology and Applications (AITA), p. 271 (1997).
[35] R. Bracewell, The Fourier Transform and its Applications, McGraw-Hill, USA, 1965; p. 1.
[36] K.R. Castleman, Digital Image Processing, Prentice-Hall, New Jersey, USA, 1996; p. 1.
[37] T. Sakagami, S. Kubo, Journal of Infrared Physics & Technology, **43**, 211 (2002).
[38] L.D. Favro, X. Han, ASNT TONES **1**, 399 (1998).